# Experimental Investigation of Turbulence Properties in Transonic Shock/Boundary-Layer Interactions

Jean M. Délery*
*Office National d'Etudes et de Recherches Aérospatiales, Châtillon, France*

**Three flows resulting from shock wave/turbulent boundary-layer interactions occurring in a two-dimensional transonic channel have been investigated. The first flow corresponds to incipient shock induced separation, the second to a well separated case, the third to a situation where a large separated bubble forms. The flows were characterized by using two-color laser velocimetry. The results include, for the three flows, mean velocity and Reynolds stress distributions across the viscous layer. The turbulence measurements reveal that the first part of the interaction process entails a very large turbulence production with the development of a very strong anisotropy. In this zone, the neglect of normal stresses in the momentum and turbulence energy equation is not justified. The downstream relaxation toward a new equilibrium state is a very gradual process due to the long lifetime of the large structures which formed in the region of intense turbulence production.**

## Nomenclature

$a$ = speed of sound
$b$ = channel width
$C_\tau$ = maximum shear stress coefficient, $2\tau/\bar{\rho}_e\bar{u}_e^2$
$H_i$ = incompressible shape parameter
$J$ = equilibrium shape parameter, $1-1/H_i$
$k$ = turbulent kinetic energy, $\frac{1}{2}(\langle u'\rangle^2+\langle v'\rangle^2+\langle w'\rangle^2)$
$M$ = Mach number
$p$ = pressure
$R$ = reattachment point
$S$ = separation point
$T$ = absolute temperature
$u$ = velocity component in streamwise direction
$v$ = velocity component in normal direction
$w$ = velocity component in cross-stream direction
$X$ = coordinate in the streamwise direction
$\bar{X}$ = reduced streamwise coordinate, $(X-X_0)/(\delta_0^*)$
$Y$ = coordinate in the normal direction
$\delta$ = dissipative layer thickness
$\delta^*$ = displacement thickness
$\rho$ = fluid density
$\tau$ = Reynolds shear stress, $-\bar{\rho}\overline{u'v'}$

*Subscripts*

$e$ = edge of dissipative layer
$t$ = stagnation condition
$0$ = origin of interaction

*Superscripts*

$(\ )'$ = fluctuating quantity
$(\bar{\ })$ = time-averaged quantity
$\langle'\rangle$ = rms value of quantity

## Introduction

VISCOUS effects play a major role in transonic flows where they can strongly affect the whole flowfield. This problem is especially important in supercritical flows where the strong viscous interaction occurring near the shock root entails a rapid thickening of the boundary layer and can lead to its separation if the shock is strong enough. These phenomena are encountered in many domains of practical interest: wings and airfoils, turbomachines, helicopter blades, etc. This fact explains the sustained effort to develop accurate predictive methods able to cope with this very difficult problem. Two kinds of approaches are followed at the moment.

1) Interaction techniques where an inviscid external flowfield and dissipative layers (boundary layers and/or wakes) are computed separately and made compatible through matching conditions. In these techniques, the dissipative layers are frequently computed by integral methods applied to boundary-layer type equations. These procedures have achieved some success, even in the case of moderately separated flows, with relatively short computer time.[1]

2) Numerical solution of the full Navier-Stokes equations, which seem the most appropriate procedure to predict the flow structure in regions where the use of the Prandtl's equations is questionable (shock root, separation region, trailing edge).

Considerable advances have been made in the development of efficient and accurate numerical codes which solve the Navier-Stokes equations. However, the numerous and systematic applications made in transonic and/or supersonic flows involving shock wave/turbulent boundary-layer interaction (SW-TBLI) have frequently led to very poor agreement with experiment, especially when separation occurs.[2-6] This inability to accurately account for viscous effects is primarily due to the deficiencies of the models employed to describe the turbulence properties of the flow. In fact, all the models tested (algebraic as well as multi-equation models) are appropriate for boundary layers undergoing relatively weak pressure gradients; however, none seem able to describe the nonequilibrium conditions typical of a shock induced separation. To define more realistic turbulence models, precise quantitative measurements of the turbulence properties are needed.

This paper presents data on three SW-TBLI's produced in a transonic channel flow and ranging from the incipient shock induced separation situation to the largely separated flow condition. The data consist of mean velocity and Reynolds stress tensor components obtained with a two-color laser velocimeter.[7]

## Experimental Arrangement

The experiments were conducted in the S8 transonic channel of the Fluid Mechanics Laboratory. This wind tunnel is continuously supplied with dessicated atmospheric air, with

Presented as Paper 81-1245 at the AIAA 14th Fluid and Plasma Dynamics Conference, Palo Alto, Calif., June 23-25, 1981; submitted July 14, 1981; revision received May 18, 1982. 

*Deputy Division Head, Aerodynamics Direction.

the stagnation conditions as follows: pressure $p_t = 95$ kPa; temperature $T_t = 300$ K. The test section, shown in Fig. 1, has a span $b$ equal to 120 mm and an entrance height of 100 mm. Interchangeable nozzle blocks or bumps can be mounted in the working section with a view to accelerating the flow up to slightly supersonic velocities. A second throat, of adjustable cross section, is placed at the test section outlet making it possible both to produce, by choking effect, a shock wave whose position, and hence intensity, can be adjusted in a continuous and precise manner; and to isolate the flowfield under study from pressure perturbations emanating from downstream ducts. Such a device notably reduces shock oscillations.

The SW-TBLI phenomena under investigation take place on the lower wall of the channel at a station where the undisturbed turbulent boundary layer has a thickness $\delta_0$ of several millimeters (from 3 to 5 mm).

The "aspect ratio" $b/\delta_0$ is approximately equal to 30. This value seems high enough to minimize three-dimensional effects in the case of flows a and b (see the following) where the thickening of the boundary layer during the interaction process is moderate.

When a large separated region forms, the local ratio $b/\delta$ decreases more significantly; for flow c, $b/\delta$ is approximately equal to 8 at reattachment. In this case, oil flow visualizations show a rather strong distortion of the reattachment line. However, the presence of three-dimensional effects is not thought to alter radically the general features of the flow and the behavior of turbulence.

Thus, the information obtained can be used as a guide to improve the modeling of two-dimensional flows. On the other hand, they can be helpful to test three-dimensional Navier-Stokes codes.[8,9]

## Results and Discussion

### Mean Flow Properties

Three SW-TBLI's, considered as typical, have been analyzed. The corresponding distributions of the "wall" Mach number $M_w$ are plotted in Fig. 2 ($M_w$ is computed from wall pressure measurements assuming an isentropic relationship and considering the stagnation pressure as constant and equal to its upstream value. The reduced streamwise distance $\tilde{X}$ is evaluated from the start of interaction $X_0$ and scaled to the boundary-layer displacement thickness at $X_0$). The locations of the transverse explorations made across the dissipative layer are also indicated in Fig. 2.

*Flow a: Interaction Corresponding to Incipient Shock Induced Separation ($M_{e_0} = 1.3$ IS)*

For this case, the test section was equipped with a symmetrical converging-diverging supersonic nozzle whose contour was designed to produce a uniform flow having a nominal Mach number equal to 1.4. The quasinormal shock wave is situated near the end of the diverging part of the nozzle at a station where the Mach number $M_{e0}$, at the boundary-layer edge, is equal to 1.30. The values of $M_{e0}$ and $H_{i0}$, in the present case, correspond to a situation which nearly coincides with incipient shock induced separation.[10]

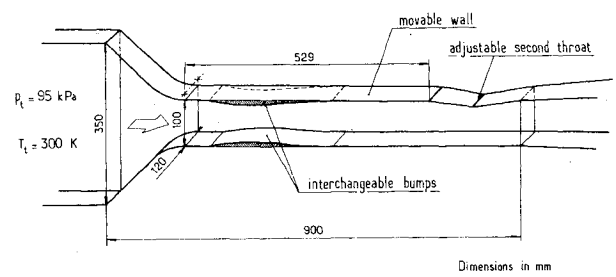


**Fig. 1 Experimental arrangement.**

*Flow b: Interaction with Separation ($M_{e_0} = 1.45$ S)*

Now, the supersonic flow is produced by a symmetrical nozzle having a nominal Mach number of 1.6. The shock wave is at a location in the nozzle leading to a Mach number $M_{e0}$ at the start of interaction equal to 1.45, thus a rather large separated bubble is formed.

*Flow c: Interaction with Extended Separation ($M_{e_0} = 1.37$ LS)*

Here, the transonic flow is produced in an asymmetrical channel where a bump is mounted on the lower wall of the wind-tunnel test section (the geometrical definition of this bump can be found in Ref. 11). The shock wave takes place at a location where the maximum Mach number in the flow is equal to 1.42. The shock is strong enough to induce boundary-layer separation upstream of the bump trailing edge. An extended separation bubble forms due to the wall curvature effect as is evidenced by the plateau of the wall pressure distribution.

Some of the mean streamwise velocity profiles measured across the dissipative layers are shown in Figs. 3a and 3b. They concern flows a and c which are the most typical. Here $Y$ is the distance from the horizontal plane which contains the flat downstream part of the test-section wall. The streamwise component $\tilde{u}$ is scaled to the value of $\tilde{u}$ at the boundary-layer edge. The bump surface has been sketched on the figures and the profiles extrapolated to the wall value by a broken line, which is only a visual aid.

For flow a (incipient separation) one observes, at first, a strong destabilization of the profiles which entails an important decrease of $\tilde{u}$ in the vicinity of the wall; yet, no negative mean values were measured. If separation actually occurs, it concerns a very small fraction of the flow too close to the wall to be detected by the present measurements. The maximum retardation effect is observed at station $\tilde{X} = 56$; downstream, turbulent viscous forces entail a gradual acceleration of the fluid in the inner part of the boundary layer. The thickness $\delta$ of the boundary layer is increasing continuously during the whole process.

In flow b (separation), a noticeable reversed flow region is formed which extends from $\tilde{X} = 18$ to 132. The thickening of the dissipative layer is now much more important than in the previous case. (The velocity profiles for this case can be found in Ref. 7.)

In the third configuration (large separation), a large separated bubble exists with a maximum reduced negative

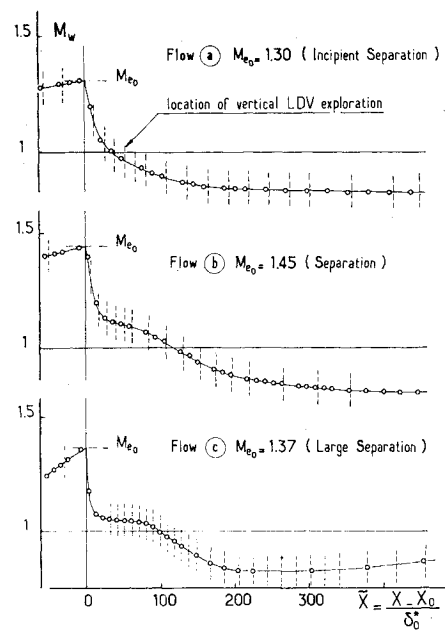


**Fig. 2 "Wall" Mach number distributions.**

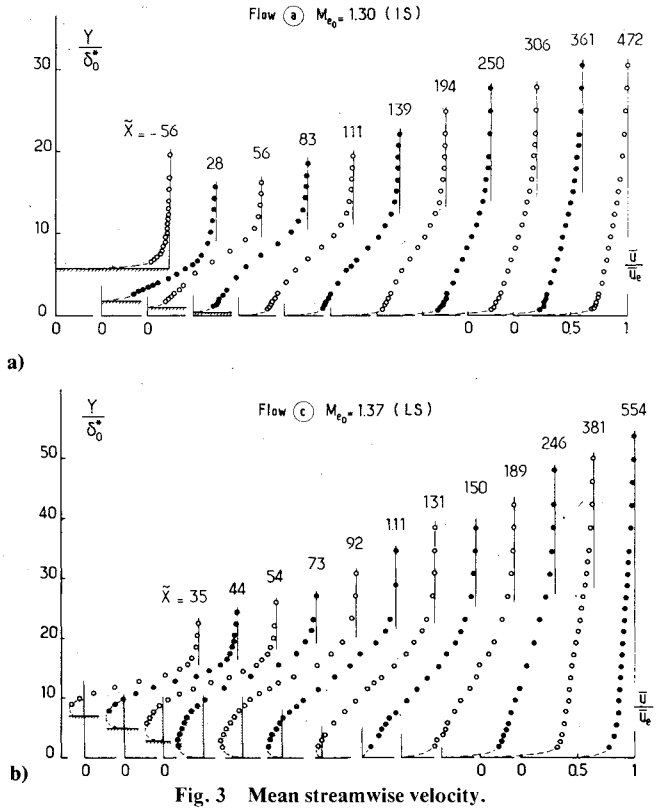


Fig. 3 Mean streamwise velocity.

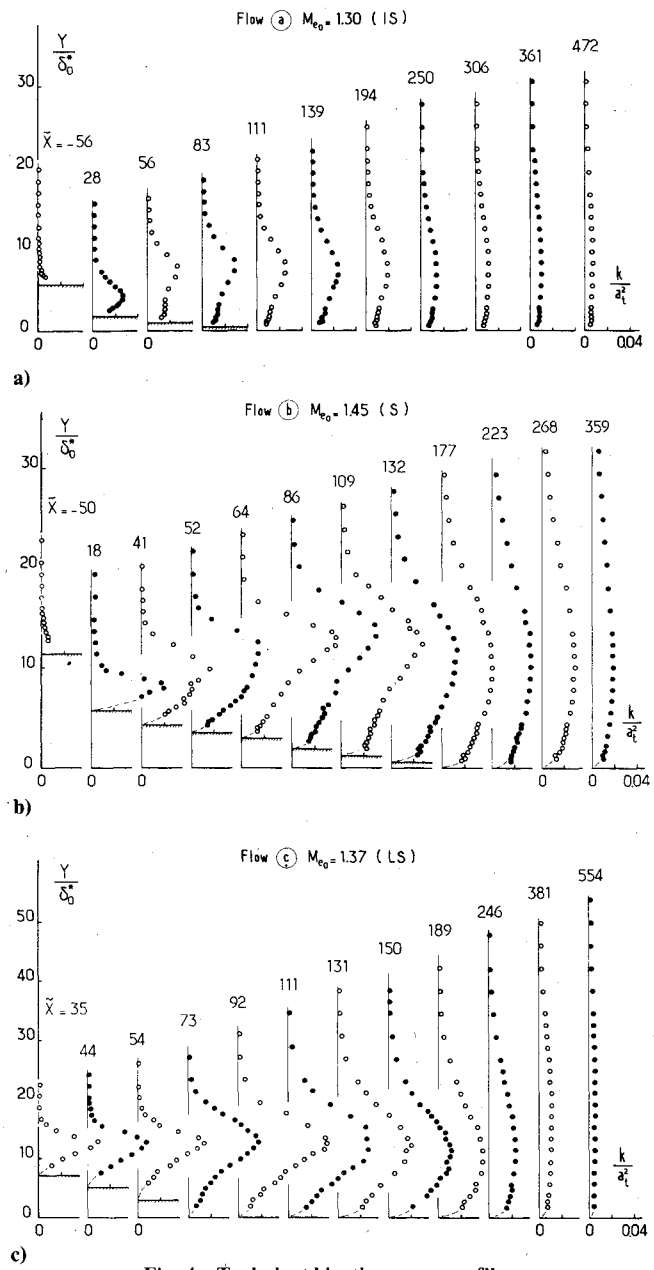


Fig. 4 Turbulent kinetic energy profiles.

velocity approximately equal to 0.2. The length of the bubble is comparable to the length of bubble in case b, but its normal extent is significantly greater (note the change in vertical scale in Fig. 3b). In this case, one observes a dramatic increase of the boundary-layer thickness, which is practically multiplied by ten between $X_0$ and the most downstream measuring station.

The two flows b and c lead to profiles whose shape and behavior in the streamwise direction are similar to data obtained in a subsonic reattachment behind a rearward facing step.[12,13] The tendency of $\bar{u}$ toward zero, due to the no-slip condition at the wall, takes place on a very short distance, so that the separated profiles have a wake-like shape.

The major part of the profiles behavior between separation and relaxation toward a new flat plate state, far downstream of reattachment, can be represented by a profile family function of a reduced number of parameters[11] (the Reynolds number and a shape parameter, compressibility effects being negligible). This observation is of interest for the development of predictive methods using integral forms of the boundary-layer equations.[1,14]

### Turbulent Flow Properties

The profiles of turbulence kinetic energy are represented in Figs. 4a-c. The kinetic energy $k$ has been evaluated by the formula

$$k = (\langle u' \rangle^2 + \langle v' \rangle^2 + \langle w' \rangle^2)/2$$

where $\langle w' \rangle^2$ has been taken equal to $(\langle v' \rangle^2 + \langle w' \rangle^2)/2$. For the three flows, there is a very large increase of $k$ in the first part of the interaction process, near the shock foot. The profiles exhibit an important maximum which is well detached from the wall. This behavior is still more pronounced for flows b and c, which are separated.

For compressible flows, the Reynolds shear stress is given by $-\bar{\rho}\overline{u'v'}$ (assuming that the triple correlation $\rho' u' v'$ is negligible). However, in the transonic flows under investigation, the change in $\bar{\rho}$ across the dissipative layer is small, so the distribution of $-\overline{u'v'}/a_t^2$ is nearly the same as $-\bar{\rho}\overline{u'v'}/\rho_t a_t^2$.

Thus, $-\overline{u'v'}/a_t^2$ can, for practical purposes, be interpreted as the nondimensional Reynolds shear stress. The $-\overline{u'v'}/a_t^2$ distributions are plotted in Figs. 5a-c. They are also characterized by the existence of a well-defined maximum, which is also well detached from the wall. For flows b and c, the maximum values of shear stress and turbulent kinetic energy generally coincide with the location of the maximum mean streamwise velocity gradient $\partial\bar{u}/\partial Y$. Such a coincidence is not observed for flow a in the first part of the interaction, where the maximum of $-\overline{u'v'}$ remains closer to the wall than the maximum of $k$.

In order to give a more vivid idea of the variations of the turbulent quantities during the interaction process, Fig. 6 shows the streamwise evolutions of maximum turbulent kinetic energy and Reynolds shear stress. The locations of separation $S$ and reattachment $R$, shown in Fig. 6, are approximate. They have been determined by interpolating laser measurements which were not realized close enough to the surface to allow a precise definition of these points; the uncertainty being larger for separation than for reattachment. There is a very large production of turbulence in the initial part of the phenomenon, near the shock root. This production

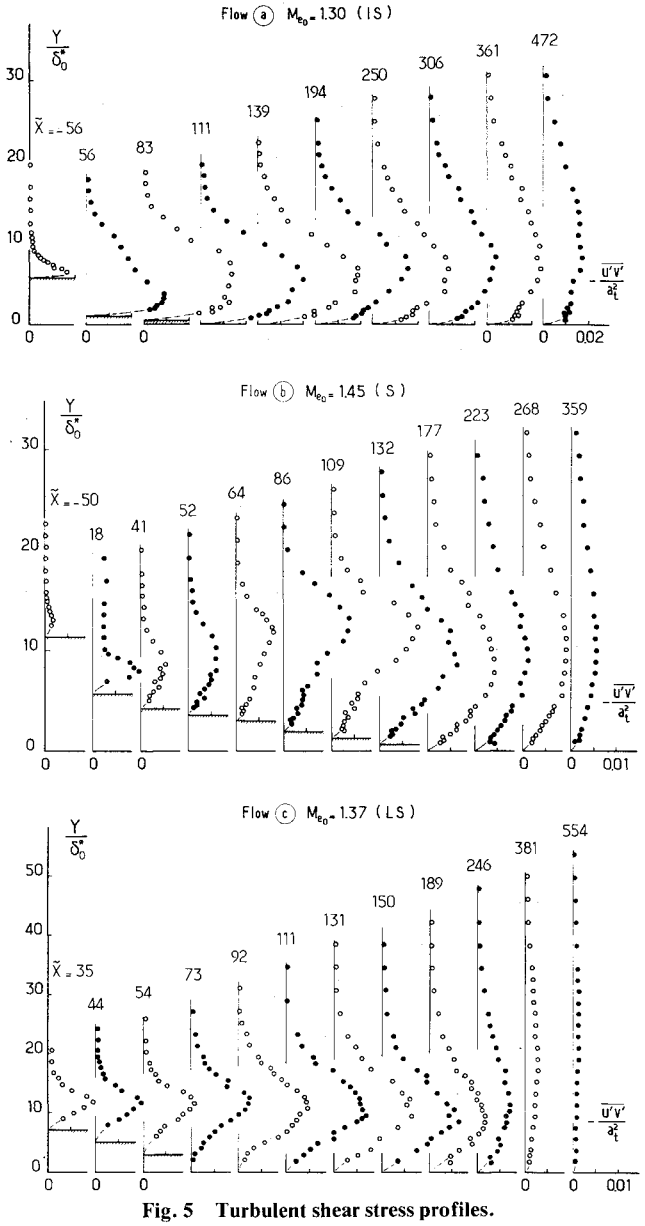


Fig. 5 Turbulent shear stress profiles.

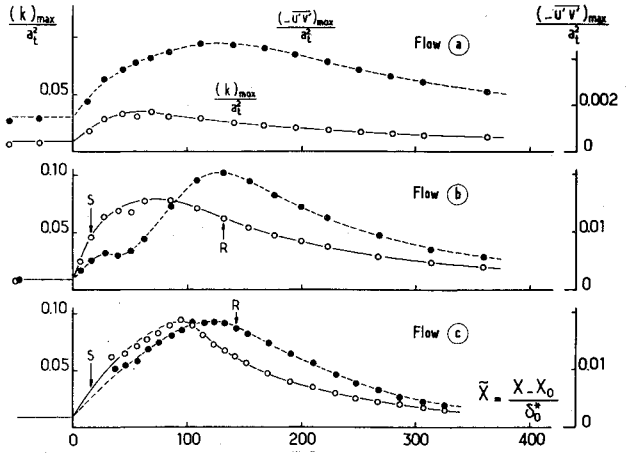


Fig. 6 Maximum kinetic energy and shear stress variation.

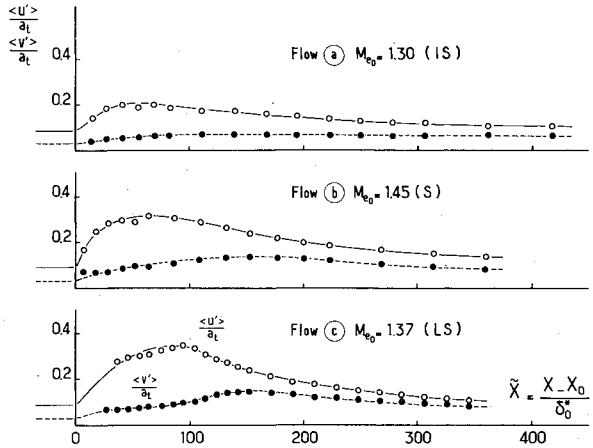


Fig. 7 Maximum turbulence intensity variation.

is enhanced when separation occurs; then $k$ tends to a maximum level, which is between eight and nine times the initial level in the undisturbed boundary layer. For flows b and c, $(k)_{max}$ starts to decrease upstream of the reattachment point $R$. Downstream of $R$, the turbulent kinetic energy diminishes rather slowly and tends gradually to a new equilibrium state. The shear stress grows at a relatively slower pace than $k$, and reaches its maximum value downstream of the point where $k$ culminates. For separated flows, the location of maximum shear stress coincides practically with the reattachment point; there, the shear stress has reached a level which is ten times the maximum initial value.

In fact, the separating boundary layer undergoes such an overwhelming perturbation that, as Bradshaw[15] postulated, the development of the free shear layer is not influenced significantly by its initial conditions, i.e., the initial boundary-layer characteristics and that production of turbulence continues in proportion to the growth of the large-scale structures until reattachment occurs.[16] Streamwise variations of the maximum rms values $\langle u' \rangle / a_t$ and $\langle v' \rangle / a_t$ are plotted in Fig. 7. In the upstream part of the interaction, the streamwise fluctuations are seen to exceed the vertical fluctuations by more than a factor of 3, in contrast to a mixing layer where $\langle u' \rangle$ is only 30% higher than $\langle v' \rangle$. Similar observations are reported in Ref. 17.

The large increase in $\langle u' \rangle^2$ is to be expected if one considers the production term of the $\langle u' \rangle^2$ transport equation (written here in the case of an incompressible flow):

$$P = -2\overline{u'v'}\frac{\partial \bar{u}}{\partial Y} - 2\langle u' \rangle^2 \frac{\partial \bar{u}}{\partial X}$$

In the first part of the interaction process, the term involving the streamwise $\bar{u}$ derivative is as large as the term involving the strain rate $\partial \bar{u}/\partial Y$ (see the following) due to the strong retardation of the whole dissipative flow. Thus, $P$ is here the sum of two large positive terms. On the other hand, the production mechanism for $\langle v' \rangle^2$ involves terms whose magnitude is far less important: $P = -2\overline{u'v'}\ \partial \bar{v}/\partial X - 2\langle v' \rangle^2 \partial \bar{v}/\partial Y$. The derivative $\partial \bar{v}/\partial X$ is small, $\partial \bar{v}/\partial Y$ is equal to $-\partial \bar{u}/\partial X$ (nearly equal for weakly compressible flows), so that the second term tends to decrease $\langle v' \rangle^2$ production in the first region where $\partial \bar{u}/\partial X$ is everywhere negative. Farther downstream, a larger and larger part of the viscous layer is accelerated, which explains the later growth of $\langle v' \rangle^2$.

Furthermore, the shear stress coefficient $(-\bar{\rho}\overline{u'v'})_{max}/\bar{\rho}_e \bar{u}_e^2$ reaches values which are significantly higher than the values for an incompressible mixing zone (0.02 instead of 0.014). Further downstream, $\langle v' \rangle$ is still increasing when $\langle u' \rangle$ has started to diminish, so that $\langle v' \rangle$ reaches its highest level well downstream of the maximum $\langle u' \rangle$ location. Proceeding further downstream $\langle u' \rangle$ and $\langle v' \rangle$ become quite comparable. The maximum fluctuation rates $\langle u' \rangle / \bar{u}_e$ for flows a, b and c, are, respectively, equal to 0.2, 0.32, and 0.38.

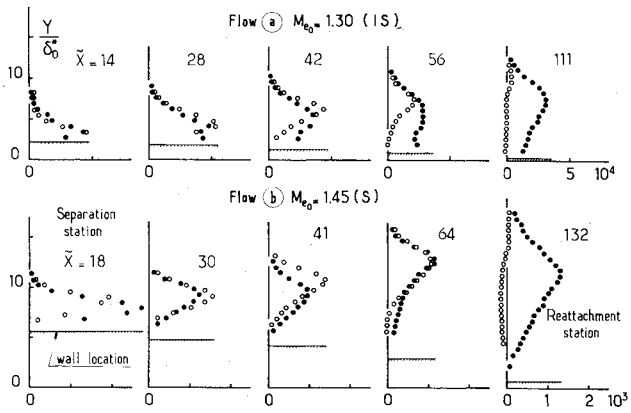


**Fig. 8 Turbulence production terms: $\bullet = -(\delta_0^*/a_i^3)\,\overline{u'v'}\,(\partial\bar{u}/\partial Y)$ and $\circ = -(\delta_0^*/a_i^3)\,(\langle u'\rangle^2 - \langle v'\rangle^2)\,(\partial\bar{u}/\partial X)$.**

Such a strong anisotropy of the flow can play a significant role in the mechanism of turbulence kinetic energy production. For an incompressible flow, and if the term involving the derivative $\partial\bar{v}/\partial X$ is neglected, the production term of the $k$ transport equation is

$$P = -\overline{u'v'}\,\frac{\partial\bar{u}}{\partial Y} - (\langle u'\rangle^2 - \langle v'\rangle^2)\,\frac{\partial\bar{u}}{\partial X}$$

The first term, representing production by shear stress, is generally predominant in shear layer and/or boundary-layer type flows and frequently is only retained in predictive methods. The two production terms have been evaluated for flows a and b for which data in the very first part of the interaction are available.

The results thus obtained are represented in Fig. 8. One notices that production due to normal stresses is as high as production due to shear stress over a streamwise distance which is of the order of 5 $\delta_0$ and which grossly corresponds to the region of steepest axial pressure gradient, where there is a general retardation of the flow ($\partial\bar{u}/\partial X<0$). Further downstream, the normal stresses contribution becomes rapidly negligible.

Let us now consider another important feature of the flow in the shock region. It is the necessity to take into account the Reynolds normal stresses in the momentum equation. The terms involving Reynolds stresses are, for an incompressible flow,

$$-\frac{\partial}{\partial Y}(\overline{u'v'}) - \frac{\partial}{\partial X}[\langle u'\rangle^2 - \langle v'\rangle^2]$$

These two derivatives have been evaluated for flows a and b. For these calculations, we have considered the flow as incompressible. This simplification does not change significantly the conclusions because of the small variation of $\bar{\rho}$ across the viscous layer ($\bar{\rho}_e/\bar{\rho}_w = 0.83$ for $M_e = 1$) and because of the relatively high uncertainty of this kind of calculations, which involve differentiation of experimental data.

It was seen (see Ref. 7) that, in the very first part of the interaction process, the $X$ derivative of normal stresses can be higher than the shear stress $Y$ derivative. Relatively far downstream, the normal stresses influence becomes negligible. Simpson et al.[18] made similar observations near the separation of an incompressible turbulent boundary layer and also showed that the neglect of the normal-stress term in the momentum and turbulence energy equations is not justified in this region.

The whole history of the interacting dissipative layer can be schematically depicted by plotting the square root of the maximum shear stress coefficient $C_\tau$ against the equilibrium shape parameter $J = 1 - 1/H_i$. Following East et al.,[19] a function $G$ based on the maximum shear stress can be defined

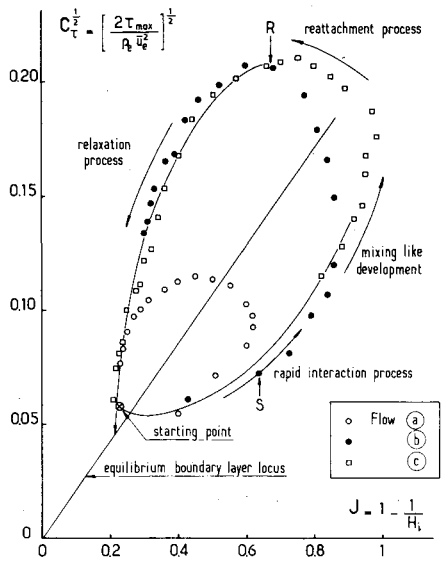


**Fig. 9 Evolution of the maximum shear stress with the equilibrium shape parameter.**

which will be constant for all equilibrium incompressible boundary-layer flows and equal to the flat plate value. Thus,

$$G = (H_i - 1)/H_i\sqrt{C_\tau/2} = 6.55$$

specifies the straight line in Fig. 9. If one plots $\sqrt{C_\tau}$ against $J$ for the present flows, the experimental points fall below the equilibrium locus in the first part of the interaction, indicating that, during this rapid interaction process, there exists a departure from equilibrium characterized by a lag of the shear stress. Then, as a consequence of the continuous increase of $C_\tau$, whereas $J$ passes through a maximum and then diminishes, the corresponding curves bend and cross the equilibrium locus at a point whose location is a function of the intensity of the destabilization process. Thereafter, the points are above the equilibrium locus and reach a new situation of maximum departure from equilibrium. Downstream of this station, and in the absence of external perturbation (no pressure gradient), the flows relax toward a new equilibrium state. In the course of this process, the representative points follow a common trajectory which leads to the equilibrium locus.

## Conclusion

A study of shock wave/turbulent boundary-layer interaction was undertaken in order to provide guidance for turbulence modeling of flows submitted to strong interaction processes. Experiments were performed with the boundary layer developing on the wall of a transonic channel. Three types of flows have been investigated; the first corresponds to an incipient shock induced separation condition, the second to a well separated case, and the third to a situation where a large separated bubble is formed. These flows have been probed by using a two-color laser velocimeter system allowing the measurement of mean velocity and Reynolds stress tensor components.

The turbulence measurements have shown that the first part of the interaction process, which corresponds to the more intense deceleration effects, entails a very large turbulence production which mainly affects the streamwise component. Initially, the flow exhibits strong anisotropy, the streamwise fluctuations exceeding the vertical fluctuations by more than a factor of 3 when there is separation. Further downstream the anisotropy of the flow diminishes gradually. Consequently, the neglect of normal stress terms in the momentum and turbulence energy equation is not justified near the shock root, where the flow is submitted to intense retardation.

During the course of interaction, the turbulent dissipative layer can be strongly out of equilibrium; one notices two maximum departures from equilibrium conditions, which are situated on each side of the equilibrium locus. The relaxation toward a new downstream equilibrium state is a rather long process due to the long life time of the large structures which formed in the region of more intense turbulence production.

The results of this study strongly suggest that only turbulence models which rely on at least one or several transport equations will be needed to represent correctly the dissipative layer behavior. Special attention has to be paid to model correctly the very first stage of the interaction, where a precise prediction of all the Reynolds stresses is essential.

## Acknowledgments

This research was made with the financial support of the Direction des Recherches et Etudes Techniques and of the Service Technique des Programmes Aéronautiques of the French Defence Ministry.

## References

[1] Le Balleur, J. C., "Calcul des écoulements à forte interaction visqueuse au moyen de méthodes de couplage," *AGARD Fluid Dynamics Panel Symposium on Computation of Viscous-Inviscid Interactions*, Colorado Springs, Colo., Sept.-Oct. 1980, AGARD-CP-291, Feb. 1981, pp. 1.1-1.36.

[2] Viegas, J. R. and Coakley, T. J., "Numerical Investigation of Turbulence Models of Shock Separated Boundary Layer Flows," AIAA Paper 77-44, Jan. 1977; see also, *AIAA Journal*, Vol. 16, April 1978, pp. 293-294.

[3] Coakley, T. J., Viegas, J. R., and Horstman, C. C., "Evaluation of Turbulence Models for Three Types of Shock Separated Boundary Layers," AIAA Paper 77-762, June 1977.

[4] Viegas, J. R. and Horstman, C. C., "Comparison of Multi-Equation Turbulence Models for Several Shock Separated Boundary Layer Interaction Flows," AIAA Paper 78-1168, July 1978; see also, *AIAA Journal*, Vol. 17, Aug. 1979, pp. 811-820.

[5] Coakley, T. J. and Bergmann, M. Y., "Effects of Turbulence Model Selection on the Prediction of Complex Aerodynamic Flows," AIAA Paper 79-0070, Jan. 1979.

[6] Marvin, J. G., Levy, L. L. Jr., and Seegmiller, H. L., "Turbulence Modeling for Unsteady Transonic Flows," *AIAA Journal*, Vol. 18, May 1980, pp. 489-496.

[7] Délery, J., "Investigation of Strong Shock-Turbulent Boundary Layer Interaction in 2D-Transonic Flows with Emphasis on Turbulence Phenomena," AIAA Paper 81-1245, June 1981.

[8] Shang, J. S., Buning, P. G., Hankey, W. L., and Wirth, M. C., "The Performance of a Vectorized 3-D Navier-Stokes Code on the CRAY-1 Computer," AIAA Paper 79-1448, July 1979.

[9] Kussoy, M. I., Viegas, J. R., and Horstman, C. C,, "An Experimental and Numerical Investigation of a 3-D Shock Separated Turbulent Boundary Layer," AIAA Paper 80-0002, Jan. 1980.

[10] Sirieix, M., Délery, J., and Stanewsky, E., "High Reynolds Number Boundary Layer-Shock Wave Interaction in Transonic Flow," *Advances in Fluid Mechanics, Lecture Notes in Physics No. 148*, Springer Verlag, 1981, pp. 149-214.

[11] Délery, J., "Analyse du décollement résultant d'une interaction choc-couche limite en transsonique," *La Recherche Aérospatiale*, No. 1978-6, Dec. 1978, pp. 305-320 (English translation ESA-TT 560).

[12] Tani, I., Iuchi, M., and Komoda, H., "Experimental Investigation of Flow Separation Associated with a Step or a Groove," Aeronautical Research Institute, University of Tokyo, Rept. 364, April 1961.

[13] Le Balleur, J. C. and Mirande, J., "Etude expérimentale et théorique du recollement bidimensionnel turbulent incompressible," *AGARD Fluid Dynamics Panel Symposium on Flow Separation*, Göttingen, Germany, May 1975, AGARD CP-168, Nov. 1975, pp. 17.1-17.13.

[14] Altstatt, M. C., "An Experimental and Analytic Investigation of a Transonic Shock-Wave/Boundary Layer Interaction," Arnold Engineering Development Center, Air Force Systems Command, Arnold Air Force Station, Tenn., AEDC-TR-77-47, May 1977.

[15] Bradshaw, P. and Wong, F.Y.F., "The Reattachment and Relaxation of a Turbulent Shear Layer," *Journal of Fluid Mechanics*, Vol. 52, Pt. 1, 1972, pp. 113-135.

[16] Seegmiller, H. L., Marvin, J. G., and Levy, L. L. Jr., "Steady and Unsteady Transonic Flow," *AIAA Journal*, Vol. 16, Dec. 1978, pp. 1262-1270.

[17] Johnson, D. A. and Bachalo, W. D., "Transonic Flow about a Two-Dimensional Airfoil—Inviscid and Turbulent Flow Properties," AIAA Paper 78-1117, July 1978; see also, *AIAA Journal*, Vol. 18, Jan. 1980, pp. 16-24.

[18] Simpson, R. L., Strickland, J. H., and Barr, P. W., "Features of Separating Turbulent Boundary Layer in the Vicinity of Separation," *Journal of Fluid Mechanics*, Vol. 79, Pt. 3, 1977, pp. 553-594.

[19] East, L. F. and Sawyer, W. G., "An Investigation of the Structure of Equilibrium Turbulent Boundary Layers," *AGARD Fluid Dynamics Panel Symposium*, The Hague, Netherlands, Sept. 1979, AGARD CP-271, Jan. 1980, pp. 6.1-6.19.